A new control system for fast motion control of SMA actuator wires

Yee Harn Teh† § and Roy Featherstone†

† Dept. Systems Engineering, Research School of Information Sciences and Engineering, The Australian National University, Canberra, ACT 0200, Australia

Abstract. This paper describes a new motion control system for actuators based on antagonistic-pair arrangements of electrically-heated SMA elements. Two different controllers have been tested, both of them incorporating a new rapid heating strategy that greatly increases the rate at which the elements can be heated without risk of overheating. Essentially, the current applied to the element is the lesser of two quantities: a desired heating current and a maximum safe current. The former is computed by a motion control law, and is a function of the position error. The latter is a function of the measured SMA resistance and predetermined threshold values. This strategy relies on the martensite and austenite phases having different resistivities, so that a range of resistance values can be identified for individual SMA elements which imply that these elements are strictly below their maximum operating temperature. Whenever the measured resistance lies within this range, a large heating current may be applied. If the resistance lies outside this range then the heating current must be cut back to a value that will not overheat the SMA. Experimental results are presented to confirm that this strategy can greatly increase the velocity of controlled motion without changing the cooling regime.

1. Introduction

Shape memory alloys (SMA) have a variety of uses both in robotic and non-robotic applications. For example, their non-robotic applications include couplings and fasteners, as well as uses in fashion, decoration and gadgets [1]. Their robotic applications include actuators in active endoscopes [2], robotic actuators [3, 4, 5] and micro-actuators [6, 7]. Their advantages include mechanical simplicity, high power-to-weight ratio, small size, and silent, spark-free operation. However, some of their disadvantages are inefficiency, hysteresis and they are generally considered to be slow.

In robotic applications, factors such as speed, accuracy, controllability and the ability to have continuous motion are very important. For this reason, SMA-based actuators are typically arranged as antagonistic pairs. They are heated by joule heating, which is by passing an electrical current through the element, and cooled by heat transfer to the environment. It is therefore the heating and cooling regimes that determine the speed of response of SMA actuators. Various researches have been conducted

§ To whom correspondence should be addressed (yee.teh@syseng.anu.edu.au)

to investigate SMA-based actuators in fast and accurate motion control applications [8, 9, 10, 11].

To increase the speed of actuators by increasing the cooling rate, forced-air cooling, forced-water cooling or using thinner SMA elements can be applied. On the other hand, to increase the heating rate, the only method is to pass a larger current through the element. However, the SMA element runs the risk of overheating, and therefore damage, if a current beyond a certain safe value has been applied for a sufficiently long duration. This safe value can often be found in an SMA data sheet.

Normally, an SMA element is heated by means of a current not exceeding the known safe current level, to avoid overheating. To further improve the speed, Kuribayashi [12] proposed monitoring the temperature of the SMA and using this information to determine the level of current to pass through the actuator. He directly measured the temperature of the SMA element using a miniature thermocouple. If the temperature is above a preset threshold, the heating current is set to zero. Otherwise, a large heating current is applied. The result of incorporating this temperature feedback mechanism is a large improvement in actuator response times.

Alternatively, the resistance of SMA elements varies during the phase transformation, and this information can be used to replace the temperature feedback mechanism proposed by Kuribayashi. The advantage of this strategy is that it eliminates the need to install special, miniature temperature sensors to determine the state of the SMA.

We propose using the resistance measurement feedback incorporated as a current limiter mechanism in a motion control system [13]. Two different motion controllers have been considered. The first is based on Grant's two-stage relay controller [8] and the second a modified proportional controller. Results showed that the speed of response had been increased compared to when the current limiter mechanism was not in place. Experimental results also show that the current limiter can be used to increase the speed of SMA actuators with different motion controllers. Results also show that the limit cycle is a manifestation of the motion controllers used and if a sufficiently good motion controller is used, such as the modified proportional controller, the limit cycle can be further reduced.

In this paper, we describe the principle of operation of the new method, the experimental hardware used to test it, and experimental results from the motion controllers showing the resulting improvement in speed and accuracy.

2. Principle of Operation

In a typical shape memory alloy, the phase transformation between the two phases, martensite and austenite, is accompanied by variations in its resistivity. This change in electrical resistance can be as high as 20%, in an alloy like nitinol. This phenomenon has been studied and has also been used to estimate the martensite ratio of the alloy during a phase transition [2, 14].

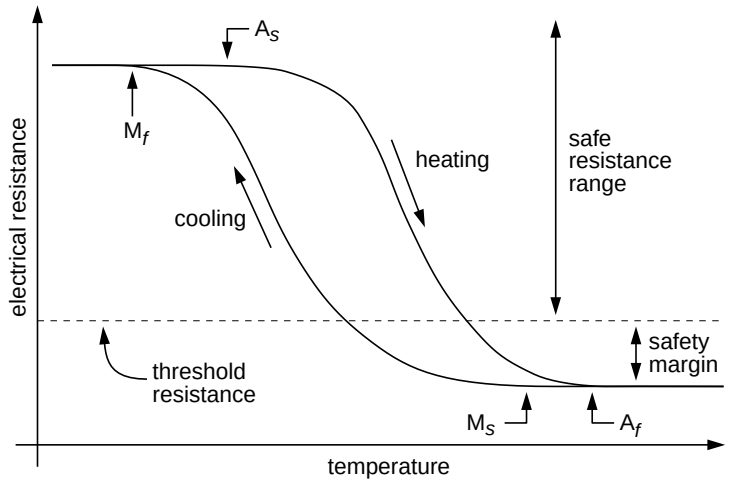

Figure 1. Typical plot of resistance versus temperature for nitinol.

Figure 1 shows a simplified plot of resistance versus temperature for a shape memory alloy such as nitinol during a phase transformation from martensite to austenite and back again. Below the martensite finish temperature, M_f, the alloy is completely in the martensite state. As it is heated from cold, it begins to transform into austenite at the austenite start temperature, A_s, and is completely in the austenite state at A_f, the austenite finish temperature. During this transition, the electrical resistance of the alloy also decreases. As the alloy is cooled from a hot state, it transforms back into martensite between the martensite start and finish temperature, M_s and M_f, together with a rise in resistance back to its original state.

Although we cannot determine the exact temperature of the alloy from its resistance, we can however identify a threshold resistance, R_{thresh}, as a boundary between the SMA 'safe' state and its 'possibly unsafe' state. In our experiments, this value has been empirically determined as the resistance of the SMA element at a temperature slightly above A_f, plus a safety margin that takes into account resistance measurement errors as well as strain-induced resistance changes.

Based on this resistance measurement, we have proposed the following current limiter mechanism that allows greater input current when the resistance is in the safe range, but limits the current when the resistance is in the unsafe regime.

2.1. Current Limiter

If an SMA actuator is heated indefinitely using a current beyond the safe level specified in its data sheet, it may run the risk of overheating the alloy. However, to implement faster motion control of SMA, we can improve the heating regime using the electrical resistance variation in SMA and the scheme in Figure 2.

Given the threshold, R_{thresh}, we define a maximum safe heating current, $I_{max}(R)$, which is a function of the measured resistance, R, as shown in Figure 2. When the SMA element resistance is below R_{thresh}, I_{safe} is applied. This value is defined as a current

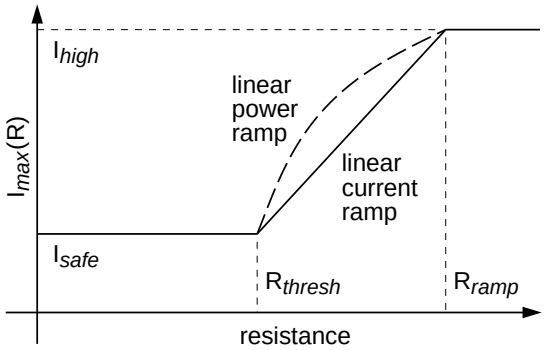

Figure 2. Maximum safe current, $I_{max}(R)$, vs. SMA element resistance, R.

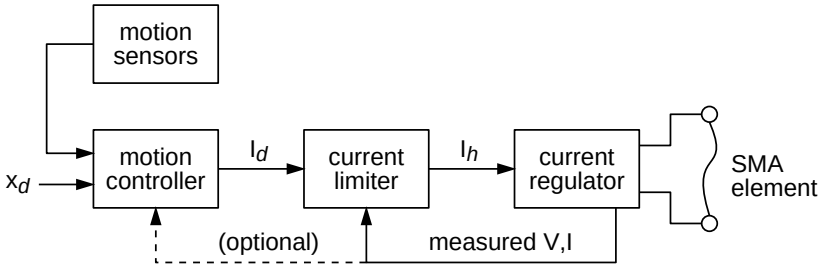

Figure 3. Motion control system with current limiter.

that can be safely applied to the element indefinitely without the risk of overheating. For example, the I_{safe} value for a $100\mu m$-diameter Flexinol wire is 0.18 A in ambient air. When the SMA element resistance is above R_{thresh}, it is safe to apply a current much larger than I_{safe}, at least for a short period of time. The upper limit, I_{high}, is determined by the current available from the power supply, or from the current regulator. The two ramps shown in the figure are optional and the purpose is to allow a smoother transition between I_{safe} and I_{high}. If a ramp is not required, then $I_{max}(R)$ would form a discontinuous function of SMA resistance, given by :

$$I_{max}(R) = \begin{cases} I_{high} & \text{if } R \geq R_{thresh} \\ I_{safe} & \text{otherwise.} \end{cases} \tag{1}$$

2.2. The Control System

Figure 3 shows a diagram of the control system incorporating the current limiter mechanism which we have implemented. Using the desired position signal, x_d, and actual position signals from one or more motion sensors, the motion controller determines an output signal, I_d. This signal can be interpreted as the desired heating current for a particular SMA element. If there are more than one SMA element, the motion controller will compute an output signal for each element, but only one such signal is shown in Figure 3. This signal is input to a current limiter that calculates the actual heating current, I_h, according to the formula:

$$I_h = \min(I_d, I_{max}(R)) \,. \tag{2}$$

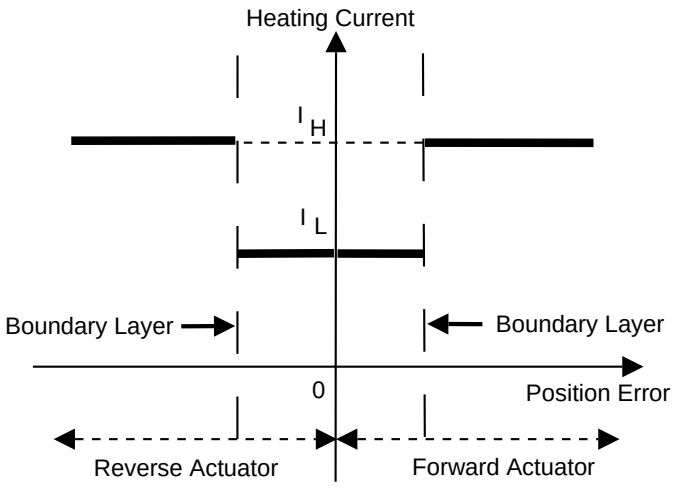

Figure 4. Two-stage relay controller.

The current regulator then passes a current of I_h through the SMA element. The actual voltage across the SMA and the actual current through it are measured and sent to the current limiter so that the electrical resistance of the SMA element can be calculated. If the current regulator is sufficiently precise, feedback of the actual SMA current is not required.

Without any limit on I_d, there is a risk of overheating the SMA element. Without any knowledge of the current state of the SMA, the only safe current-limiting strategy is to have I_d less than or equal to I_{safe}. The rapid heating method allows larger heating currents to be applied without risk of overheating.

We have investigated the behaviour of our rapid heating algorithm with two motion control laws: a two-stage relay controller and a modified proportional controller. These are described below.

2.3. Two-Stage Relay Controller

Grant's two-stage relay controller [8] implements the control law scheme as shown in Figure 4. At any instant, only one SMA element is being heated, depending on the sign of the position error. It uses two constant magnitude heating currents to drive the SMA elements. The following control law is implemented:

$$(I_{Fd}, I_{Rd}) = \begin{cases} (0, I_H) & \theta_{err} < -\phi \\ (0, I_L) & -\phi \leq \theta_{err} < 0 \\ (I_L, 0) & 0 \leq \theta_{err} < \phi \\ (I_H, 0) & \phi \leq \theta_{err}, \end{cases} \tag{3}$$

where θ_{err} is the position error, I_{Fd} and I_{Rd} are the desired heating currents for the forward and reverse SMA elements respectively, and I_H, I_L and ϕ are parameters of the controller. When the position error is large, the high current input, I_H, is used to drive the actuator quickly to the desired position. As the position error approaches zero and

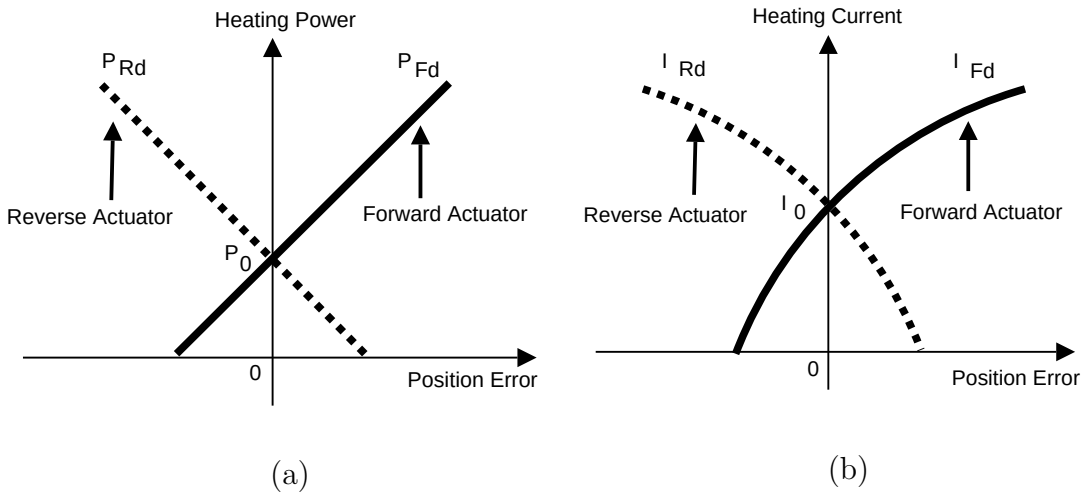

Figure 5. Modified proportional controller: heating power vs. position error, θ_{err} (a), and heating current vs. position error, θ_{err} (b).

reaches the boundary layer, ϕ, the relay controller switches to a lower current input, I_L, for smoother and more stable response. The forward and reverse SMA elements pull in the positive and negative directions, as measured by the position sensor. The desired heating currents, I_{Fd} and I_{Rd} are the inputs to two current limiters which calculate the actual heating currents to be sent to each SMA.

Note that our two-stage relay controller differs from Grant's on the magnitude of heating current. Whereas Grant used I_{safe} as I_H, we set I_H to a value greater than the safe current level.

2.4. Modified Proportional Controller

The modified proportional controller algorithm is depicted in Figure 5. The controller computes a linear power ramp (Figure 5(a)) and converts the heating power, P, to current, I (Figure 5(b)), based on the following relationship:

$$I = \sqrt{\frac{P}{R_{nom}}}, \tag{4}$$

where R_{nom} is the pre-determined, nominal resistance of the SMA element.

Basically the modified proportional controller implements the following control law:

$$(P_{Fd}, P_{Rd}) = (max(0, P_0 + K_p\theta_{err}), max(0, P_0 - K_p\theta_{err})), \tag{5}$$

where θ_{err} is the position error, P_{Fd} and P_{Rd} are the desired heating powers for the forward and reverse SMA elements, respectively, K_p is the proportional gain, and P_0 is the applied heating power when θ_{err} is zero. When the error is large, only one wire is heated according to the control law. The other wire remains cold. As the error decreases, the desired heating power decreases proportionally. At a certain position error, the controller will commence supplying power to the other SMA element so that

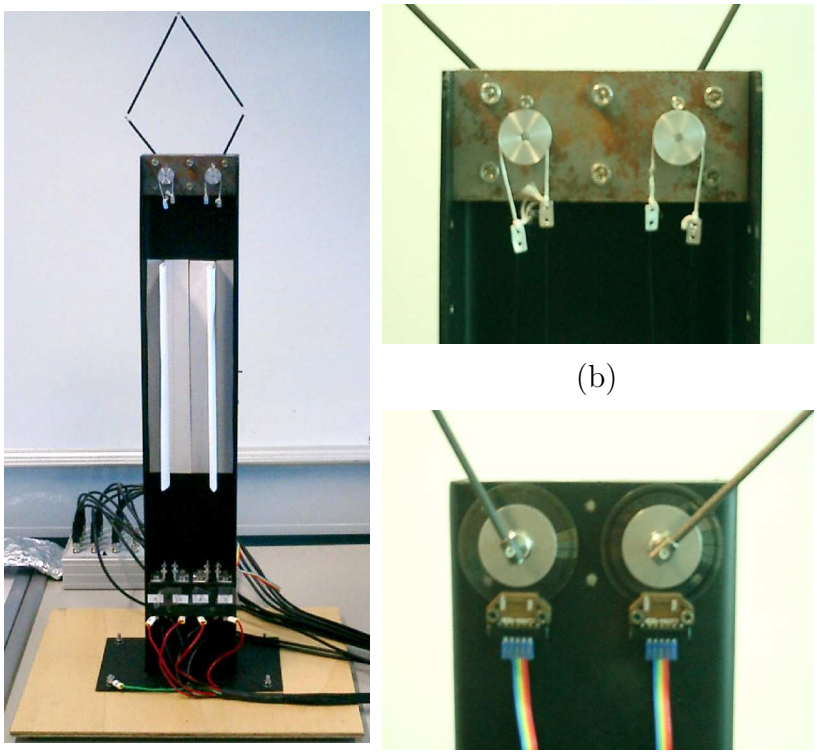

(a) (b) (c)

Figure 6. The experimental rig (a), and detailed views of the pulleys (b) and optical encoders (c).

both actuators are being heated and do not become slack. Depending on the sign of the error, one SMA element is supplied more power than the other, and actuation occurs in the desired direction.

By setting P_0 correctly (by empirical method), both elements will be supplied the same level of heating power, and remain just above the austenite start temperature, when the position error is zero. The rationale is to keep both wires taut when the position error is zero, by keeping both of them warm. This is to eliminate or to further reduce the limit cycle.

3. Experimental Setup

The experimental rig is shown in Figure 6(a) and schematically in Figure 7. It consists of a vertical steel C-beam, about 0.7m high, supporting two horizontal protruding shafts at the top and eight anchor points at the bottom. Each shaft at the top rotates freely on ball bearings and carries a small pulley at the front (Figure 6(b)) and an optical encoder wheel at the rear (Figure 6(c)). The two shafts terminate with small sockets, welded to the rear end of the each shaft, which hold the ends of a pantograph linkage made from carbon tubes. The pantograph serves as a mechanical load. Separators made of paper are affixed half way up the column to prevent the SMA elements from making electrical

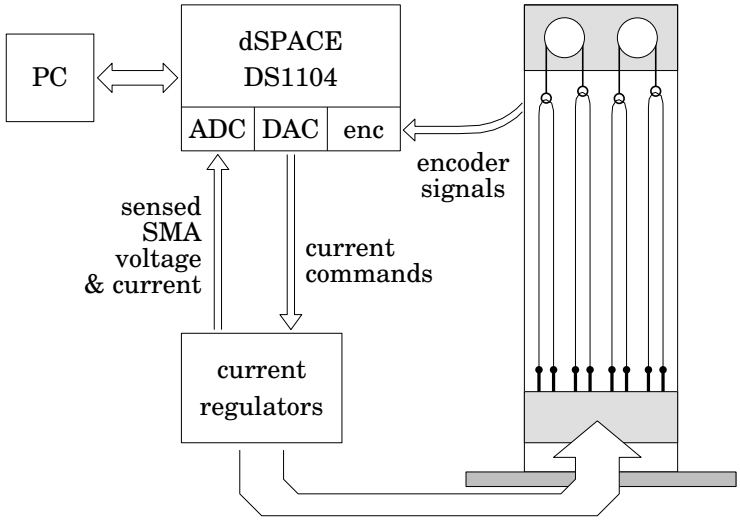

Figure 7. Schematic diagram of experimental hardware.

contact with their neighbours if they go slack.

A short chord is wrapped around each pulley and is affixed so that it cannot slip relative to the pulley. Each end of the chord terminates with a metal eyelet. Four $100\mu m$-diameter Flexinol wires are strung between the eight anchor points and the eyelets as shown in Figure 7 to form two antagonistic pairs of SMA actuators. These wires are approximately 1 m long and are too thin to be visible in Figure 6(a).

Figure 7 shows a schematic diagram of the complete experimental setup. All real-time computation and data capture functions are performed on a DS1104 board from dSpace, which communicates with a PC in the MATLAB/Simulink environment. Current regulators deliver electrical power to each SMA wires independently according to signals from the four DAC outputs of the DS1104. Each regulator is capable of supplying more than 0.65A (40W) to its load, which is more than enough to burn out the SMA wires. The actual voltage across each wire and the actual current passing through it can be measured using the current regulator circuits, and these signals are passed back to the ADC inputs on the DS1104. However, due to noise in the signals, we found it necessary to pass them through low-pass filters before we could obtain accurate electrical resistance measurements.

The optical shaft encoders are also connected to the DS1104 to provide rotation angles of each pulley from an absolute position. Based on this setup, the motion range of the pulley due to the actuation of Flexinol wires is slightly more than 90°.

4. Experimental Results

We have tested the two different controllers with the current limiter mechanism under a variety of conditions. With the relay controller, the rapid heating mechanism of the current limiter, when enabled, substantially improves the speed, but the tracking accuracy suffers from large limit cycles especially under the condition of external

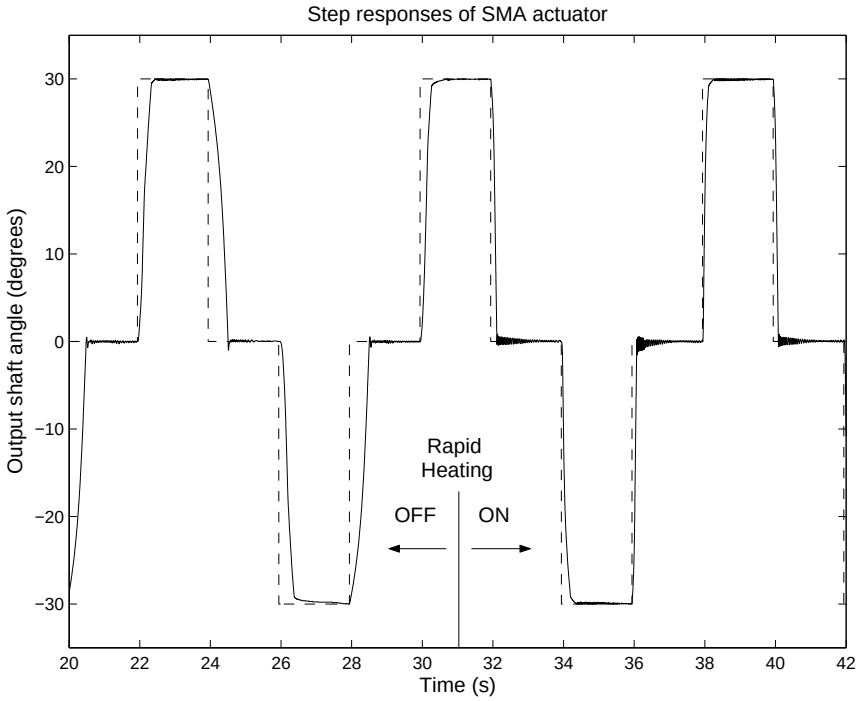

Figure 8. Tracking response (solid line) of an antagonistically actuated pulley to step position command (dashed line) under no-load conditions.

payload. The modified proportional controller manages to reduce the limit cycle problem while maintaining improvement in the speed of response.

Figures 8 and 9 clearly show the improvement in the tracking response due to the rapid heating. The 60° peak-to-peak magnitude corresponds to a 1.6% strain on the SMA wires. Both experiments were conducted under no-load conditions.

In Figure 8, before the 31-second mark, the rapid heating mechanism is effectively disabled by setting I_{high} from the current limiter to I_{safe}. During this period, the control system functions exactly like Grant's two-stage relay controller. Around the 31-second mark, the rapid heating mechanism is enabled by setting I_{high} to a high value. The larger heating currents sent to the actuators causes an immediate decrease in the rise and fall times of the step response. In terms of limit cycles, the performance is slightly worse at the steady state. This is due to the substantial increase in velocity caused by the faster heating input.

Figure 9 shows the tracking response to a 1-Hz sine wave input. Similarly, rapid heating is disabled before the 30-second mark. The controller is unable to track the sine wave accurately because the actuators move too slowly. When rapid heating is enabled, an immediate increase in actuator velocity is detected by the improved response as shown in Figure 9. The peak actuator velocity has been increased by a factor of 2, from approximately $90°/s$ to $180°/s$. However, it is still not fast enough to track the whole of the sine wave accurately.

Figure 10 shows the actual power delivered to the two SMA wires during the sine

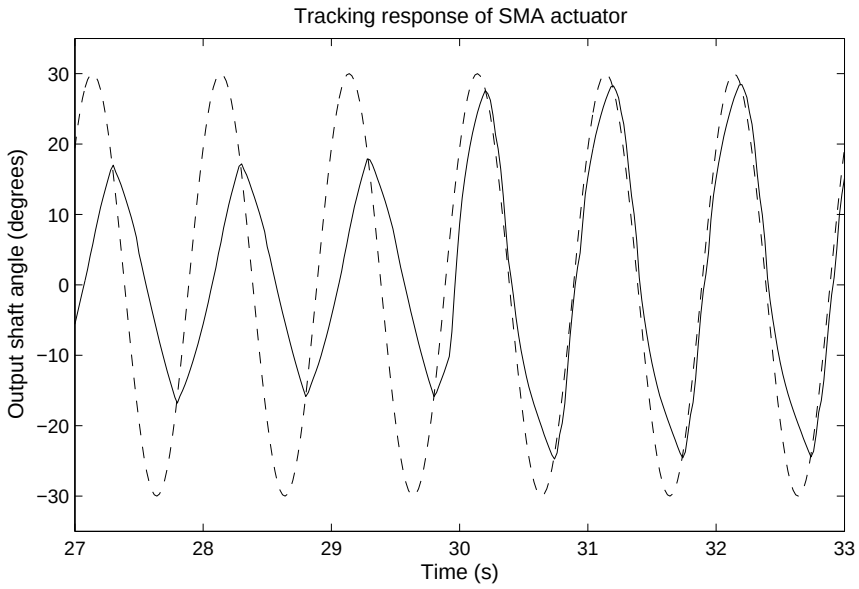

Figure 9. Tracking response (solid line) of an antagonistically actuated pulley to a 1Hz sinusoidal position command (dashed line) under no-load conditions.

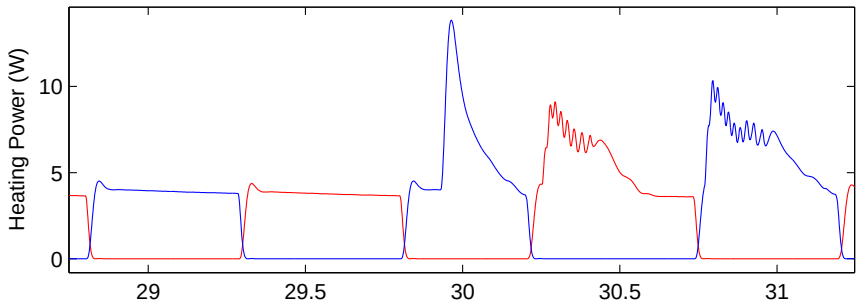

Figure 10. Actual power delivered to the two actuator wires during the motion shown in Figure 9.

wave tracking experiment of Figure 9. This actual power is computed using the SMA voltage and current measurements, which have been low-pass filtered. Prior to the 30-second mark, the heating power is at the safe level corresponding to the I_{safe} current level. The spike at the 30-second mark corresponds to the moment when the rapid heating mechanism is enabled. Based on the current limiter scheme in Figure 2, the wires are heated very rapidly using currents beyond the safe level, but the heating power decays to lower levels as the SMA wire resistance drops below the safe threshold, R_{thresh}. Similar results of speed improvement have been obtained for experiments involving the modified proportional controller.

We have also tested both motion control systems under an external load condition. A carbon tube, 0.15 m long and weighing 0.8 g, is attached to the socket at the rear end of the pulley shaft as shown in Figure 6(c). This carbon tube constitutes a difficult load to control, as there is no additional damping in the system. Its vibration causes

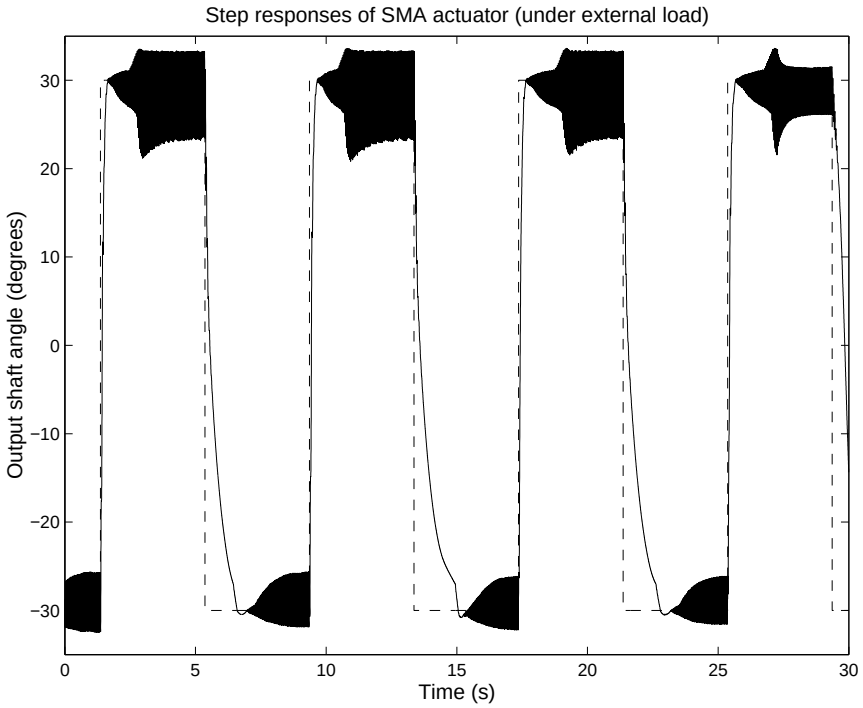

Figure 11. Tracking response (solid line) of an antagonistically actuated pulley to step position command (dashed line) under external load conditions (using two-stage relay controller).

large limit cycles as observed in our results.

The step response of the two-stage relay controller under the external load condition is shown in Figure 11. Note that the rapid heating mechanism is enabled. The response shows a noticeable limit cycle magnitude at the steady state. It also shows an asymmetry in the tracking speed when the position command switches between $+30^\circ$ and -30°. The reason for this is unknown.

Figure 12 shows the step response of the modified proportional controller after a new pair of SMA wires has been installed. It clearly shows that the large limit cycles due to the carbon tube load have been eliminated with careful tuning of the parameters, K_p and P_0. The current limiter incorporated with this controller has also effectively improved the speed of response of the SMA elements as noted in the sharp rises and falls in response to the step input signal.

5. Conclusion and Future Work

A new rapid electrical heating method of SMA elements has been proposed and described in this paper. It is based on the fact that the electrical resistance of an SMA element varies with its martensite ratio, and therefore can be used as an indication of temperature. The current limiter mechanism calculates a maximum heating current as a function of the measured element-specific resistance, which may be many times larger than the safe current level indicated on the SMA data sheet; and it ensures that the

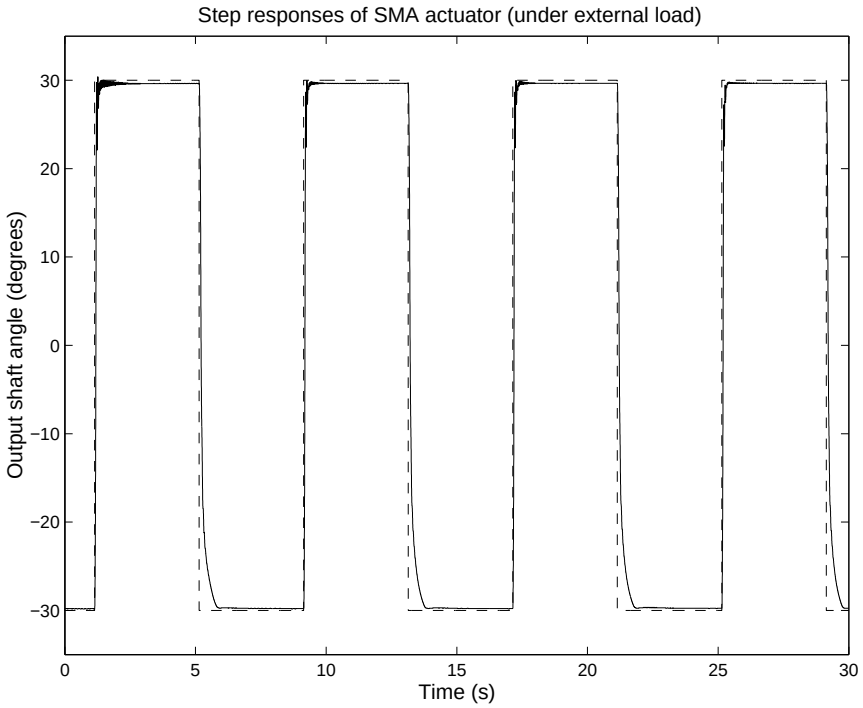

Figure 12. Tracking response (solid line) of an antagonistically actuated pulley to step position command (dashed line) under external load conditions (using modified proportional controller).

actual heating current never exceeds this calculated maximum current. This mechanism is conceptually-similar to Kuribayashi's method [12] but it dispenses with the need for special thermocouple to measure the SMA temperature.

Two different motion control systems have been incorporated with the current limiter and have been tested under different conditions to demonstrate the effectiveness of the new mechanism. Experimental results for the tracking response of an antagonistic pair of SMA wires under no-load conditions show that the current limiter has significantly improved the speed of response compared to the case where only safe current levels of heating are applied. This improvement is obtained purely by faster heating.

Under the external load condition, the relay controller performance has been degraded due to the large limit cycle problem. In order to eliminate this problem, the modified proportional controller has been designed and experimental results show that the tracking accuracy has substantially improved with the elimination of large limit cycles.

We are currently designing a new test rig that will include load cells for measuring the stress on each SMA element. Using data from the load cells, we intend to implement force control systems as well as faster and more accurate motion control systems.

References

[1] Van Humbeeck J 1999 'Non-medical applications of shape memory alloys' *Materials Science and Engineering A* **273-275** p 134-48

[2] Ikuta K, Tsukamoto M and Hirose S 1988 'Shape memory alloy servo actuator system with electric resistance feedback and application for active endoscope' *Proc. IEEE Int. Conf. Robotics & Automation* (Philadelphia, PA) p 427-30

[3] Hirose S, Ikuta K and Umetani Y 1985 'A new design method of servo-actuators based on the shape memory effect' in Morecki A, Bianchi G and Kędzior K (Eds.) *Theory and Practice of Robots and Manipulators* (Cambridge, MA: MIT Press) p 339-49

[4] Mosley M J and Mavroidis C 2001 'Experimental nonlinear dynamics of a shape memory alloy wire bundle actuator' *Trans. ASME, J. Dynamic Systems, Measurement & Control* **123** (1) P 103-12

[5] Reynaerts D and Van Brussel H 1998 'Design aspects of shape memory actuators' *Mechatronics* **8** p 635-56

[6] Troisfontaine N, Bidaud Ph and Dario P 1998 'Control experiments on two SMA based micro-actuators' in Casals A and de Almeida A T (Eds.) *Experimental Robotics V* (London: Springer) p 490-99

[7] Yao Q, Jin S and Ma P 2004 'The micro trolley based on SMA and its control system' *J. Intelligent and Robotic Systems* **39** p 199-208

[8] Grant D 1999 'Accurate and rapid control of shape memory alloy actuators' PhD Thesis, Centre for Intelligent Machines, McGill University TR-CIM-99-11

[9] Wellman P S, Peine W J, Favalora G E and Howe R D 1998 'Mechanical design and control of a high-bandwidth shape memory alloy tactile display' in Casals A and de Almeida A T (Eds.) *Experimental Robotics V* (London: Springer) p 56-66

[10] Rediniotis O K, Wilson L N, Lagoudas D C and Khan M M 2002 'Development of a shape-memory-alloy actuated biomimetic hydrofoil' *J. Intelligent Material Systems & Structures* **13** p 35-49

[11] Elahinia M H, Seigler T M, Leo D J and Ahmadian M 2004 'Nonlinear stress-based control of a rotary SMA-actuated manipulator' *J. Intelligent Materials Systems & Structures* **15** (6) p 495-508

[12] Kuribayashi K 1991 'Improvement of the response of an SMA actuator using a temperature sensor' *Int. J. Robotics Research* **10** (1) p 13-20

[13] Featherstone R and Teh Y H 2004 'Improving the speed of shape memory alloy actuators by faster electrical heating' *Proc. 9th Int. Symp. Experimental Robotics* (Singapore) Paper ID 128

[14] Kotil T, Sehitoglu H, Maier H J and Chumlyakov Y I 2003 'Transformation and detwinning induced eletrical resistance variations in NiTiCu' *Materials Science & Engineering* **359** p 280-89